LETTER • OPEN ACCESS

Decoupling the sequence of dielectric breakdown in single device bilayer stacks by radiation-controlled, spatially localized creation of oxide defects

View the article online for updates and enhancements.

Decoupling the sequence of dielectric breakdown in single device bilayer stacks by radiation-controlled, spatially localized creation of oxide defects

Fernando Leonel Aguirre[1,2] , Alok Ranjan[3] , Nagarajan Raghavan[3] , Andrea Padovani[4] , Sebastián Matías Pazos[1,2] , Nahuel Vega[5] , Nahuel Müller[5] , Mario Debray[5] , Joel Molina-Reyes[6] , Kin Leong Pey[3] , and Félix Palumbo[1,2*]

[1]Unidad de Investigación y Desarrollo de las Ingenierías, Universidad Tecnológica Nacional Facultad Regional Buenos Aires (UIDI UTN-FRBA), Medrano 951, Buenos Aires, C1179AAQ, Argentina
[2]Consejo Nacional de Investigaciones Científicas y Técnicas (CONICET), Godoy Cruz 2290, Buenos Aires, C1425FAB, Argentina
[3]Engineering Product Development (EPD) Pillar, Singapore University of Technology & Design, 8 Somapah Road, 487372, Singapore
[4]Applied Materials—MDLx, Via Meuccio Ruini 74/L, 42124, Reggio Emilia, Italy
[5]Laboratorio TANDAR—Gerencia de Investigación y Aplicaciones, Comisión Nacional de Energía Atómica Centro Atómico Constituyentes (GIyA-CNEA-CAC), Av. Gral. Paz 1499, San Martín, Buenos Aires, Argentina
[6]Instituto Nacional de Astrofísica, Óptica y Electrónica (INAOE), Tonantzintla, Puebla, 72840, Mexico

*E-mail: felix.palumbo@conicet.gov.ar

Received September 27, 2021; revised October 15, 2021; accepted October 27, 2021; published online November 10, 2021

The breakdown (BD) sequence in high-K/interfacial layer (HK/IL) stacks for time-dependent dielectric breakdown (TDDB) has remained controversial for sub-45 nm CMOS nodes, as many attempts to decode it were not based on proper experimental methods. Know-how of this sequence is critical to the future design for reliability of FinFETs and nanosheet transistors. We present here the use of radiation fluence as a tool to precisely tune the defect density in the dielectric layer, which jointly with the statistical study of the soft, progressive and hard BD, allow us to infer the BD sequence using a single HfO$_2$–SiO$_x$ bilayered MOS structure. © 2021 The Author(s). Published on behalf of The Japan Society of Applied Physics by IOP Publishing Ltd

Breakdown of ultra-thin dielectrics is one of the critical failure mechanisms that has remained a topic of intense study for the past 3–4 decades. While sufficient know-how on the physics, statistics and kinetics governing dielectric breakdown in HfO$_2$[1,2] and SiO$_X$[3] are separately known, the presence of a bi-layer stack of these in sub-45 nm technologies brought in a big element of complexity into inferring the statistical results of time dependent dielectric breakdown (TDDB) measurements. The main questions to be answered are: does the HK break down (BD) first or the IL? Is there a fixed sequence or is this sequence dependent on the process induced defect distributions, operating conditions and dielectric thickness combinations? Which of the two dielectrics should be the subject of focus of future design for reliability initiatives in the front end of line?

Several attempts to decode this sequence were explored in the past few years based on the charge transport (conduction) mechanisms,[4] dedicated two-stage TDDB test schema,[5] Kinetic Monte Carlo simulation of TDDB considering Weibull slope trends,[6] wide variations in process conditions for depositing the HK,[7] TDDB at different HK-IL thickness combinations,[8] stress induced leakage current (SILC) trends in thin and thick IL devices,[9] trend of Weibull slope changes with HK-IL thickness combinations,[10] different thermochemical bond strength and activation energy of bond-breakage[11] as well as charge pumping during SILC stress.[12] The inferences from these approaches remained unclear with some suggesting IL to break down first[5,8–12] and others pointing to the HK.[4,6,7]

In our study here, we propose a new approach to decode the sequence of BD more convincingly using a radiation fluence based experimental strategy for the selective defect introduction in the HK layer alone. A very thick HK with ultra-thin IL layer stack is chosen on purpose to induce a stark contrast in the electric field patterns and in addition to β, we use the defect clustering factor (α_C), which is a more discriminative metric to decouple the stochasticity in BD kinetics of HK and IL. The novelty of our approach lies in the use of just one device stack (one single combination of HK and IL thickness) and one stress voltage to infer the BD sequence leveraging on a calibrated radiation setup that allows for customized through thickness spatial defect density control in the HK.

Metal oxide semiconductor capacitors (MOSCAP) with area of $60 \times 60 \, \mu m^2$ were fabricated, containing a thick HfO$_2$ film deposited by atomic layer deposition at 250 °C and an Al top electrode (TE) of 400–500 μm thick. The stack consisted of 6.50–6.75 nm HfO$_2$ and 3–4 Å interfacial layer (SiO$_X$) as evident from transmission electron micrograph (TEM) [Fig. 1(a)]. To introduce defects in the stack, we use radiation fluence. SRIM simulations were executed to choose the ion species and energy of the bombarding ions. To ensure minimal displacement of atoms from their equilibrium positions, carbon ions (C^{+4}) were selected and the energy was configured to be 40 MeV, considering the dielectric thickness of the bilayer stack and the large discrepancy in atomic density of HfO$_2$ (9.64 g cm^{-2}) and SiO$_X$ (1.65–2.25 g cm^{-2}).[13] The chosen energy of C^{+4} enables defects to be solely created in the bulk of the HfO$_2$ layer, as confirmed by the particle track traces in SRIM [Fig. 1(b)], which point to a two orders of magnitude difference in the total vacancies created per ion, 2.4×10^{-2} Vo ion^{-1} for HfO$_2$ versus 7.7×10^{-4} Vo ion^{-1} in SiO$_X$. Therefore, we can assume that the radiation induced damage will occur in the HK film with negligible impact on the IL. Note that energy losses through the Al TE were also accounted for in our simulations, which turn out to be negligible (<1%). In the study, the beam spot size is adjusted to cover the whole area of the device.

Considering a typical density of intrinsic defects (N_d) in the HK, the ion fluence was back calculated. We found the
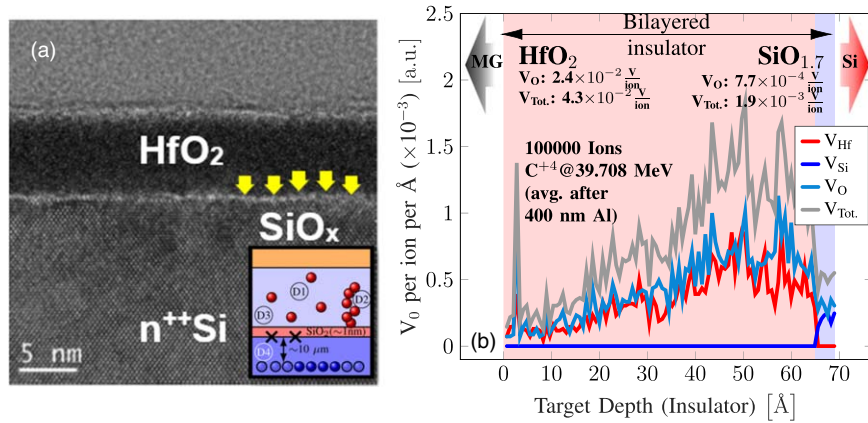
Fig. 1. (Color online) (a) TEM micrograph of the bi-layer HfO$_2$/SiO$_X$ MOSCAP stack under test. The yellow arrows point to the thin SiO$_X$ IL. The inset shows a schematic of the defect profile induced by the radiation fluence in the stack. (b) SRIM calculations showing the through-thickness profile of the radiation induced damage (oxygen vacancy creation mostly in HfO$_2$).

suitable value of C^{+4} fluence to be from 10^{11} to 10^{13} ions cm^{-2} (with three samples S1–S3, corresponding to 10^{11}, 10^{12} and 10^{13} ions cm^{-2}, respectively), enabling bulk defect densities in the range of 10^{16}–10^{18} cm^{-3}, respectively. Although even higher fluences can be chosen, they are avoided here due to their negative influence on the carrier mobility and aggravation of charge trapping, both of which increase the series resistance (R$_S$),[14] which would complicate the interpretation of the TDDB results.

The TDDB stressing was carried out using a single stress voltage of $V_G - V_{FB} = 2.4$ V with compliance, $I_{comp} \sim 1$ mA. The stress was not interrupted after the first percolation (soft BD) event, instead the dielectric was purposely stressed to examine the progressive breakdown (PBD) transient phase characterized by noisy gradual leakage current (I_{gate}) evolution all the way until the final hard BD (HBD).

Our multi-frequency capacitance-voltage (MFCV) analyses on the fresh (S0) [Fig. 2(a)] and most highly irradiated sample (S3) [Fig. 2(b)] show that the extracted flat band voltage (V_{FB}, ~-0.1 V, calculated with the "inflection point" technique[15]) and the maximal capacitance in accumulation (~ 1.2 μF cm^{-2} which agrees well with the theoretical value) remained constant. The density of interface states, D_{it}, calculated with the conductance method[16] at room temperature and in the mid-gap region also showed minimal variations—in line with the very reduced "weak inversion hump" in Fig. 2(b)—proving that defects were only introduced in the bulk of the HK and that the IL layer is largely unperturbed.

The trend of I_{gate} evolution (in the logarithmic scale) during the TDDB stress is shown in Figs. 2(c) and 2(d) for the fresh sample (S0) and most severely radiation exposed sample (S3), respectively. A few key points to note here are that the there is an initial phase of charge trapping resulting in a gradual reduction in current followed by a soft BD (SBD), that could correspond to the percolation of one of the two dielectrics in the stack. This SBD instant is followed by a prolonged phase of noisy gradual I_{gate} increase which follows a power law trend with time. This phase is categorized as PBD. After the PBD causes an increase in current by around two orders of magnitude, the final abrupt jump in current towards I_{comp}, resulting in HBD is observed. While the PBD phase could involve several factors playing a role including

the wear-out of the first percolation path and the simultaneous nucleation of many more percolation paths that may be spatially correlated/uncorrelated within the same dielectric layer, the HBD instant can be claimed to correspond to the BD of the second layer of dielectric in the stack, due to the large increase in current representing an end-to-end BD of the complete bi-layer stack.

The time to 1st SBD (t_{SBD}) and the time duration between the 1st SBD and the final HBD event ($t_{HBD} - t_{SBD} = t_{PBD}$)[17] are plotted on a Weibull scale as shown in Fig. 3(a). The durations of t_{SBD} and t_{PBD} are essentially the times taken for each of the dielectrics to suffer their first percolation event. While the duration t_{PBD} may certainly comprise several additional SBD events within the previously percolated dielectric layer and their wear-out, the thermal/field impact of these events on the other dielectric are miniscule[18] compared to the effect that the second percolation BD has on the leakage current jump (the instant of HBD). Based on the recent work of Wu et al.,[19] we consider fitting the data with the defect clustering model [Eq. (1)] which is a more generic representation of the Weibull model with a cluster factor (α_C) that characterizes the extent of spatial proximity of vacancy generation to pre-existing vacancy defects. A highly correlated defect generation process would have α_C varying between 0 and 1 while a completely random defect generation process would ideally correspond to $\alpha_C \to \infty$. In the equation below, $F_{Cluster}$ is the cumulative density function and $\{\beta, \eta\}$ carry their usual meaning of Weibull slope and 63rd percentile mean time to failure, respectively

$$F_{Cluster} = 1 - \left(1 + \frac{1}{\alpha_C}\left(\frac{t}{\eta}\right)^\beta\right)^{-\alpha_C}. \tag{1}$$

The trend of β, α_C and η (also referred to as $t_{63\%}$) as a function of the radiation fluence is plotted for the SBD and PBD stages of BD in Figs. 3(b)–3(d) for samples S1–S3, alongside the fresh non-irradiated sample, S0. The fitting was done using the standard expectation-maximization algorithm to optimize the log-likelihood function and 25 device units were considered for each sample. Note that for each parameter estimate, the 95% confidence interval is also shown. While the value of β_{SBD} remained relatively fixed at ~ 1 for SBD across all the four samples, β_{PBD} showed a significant
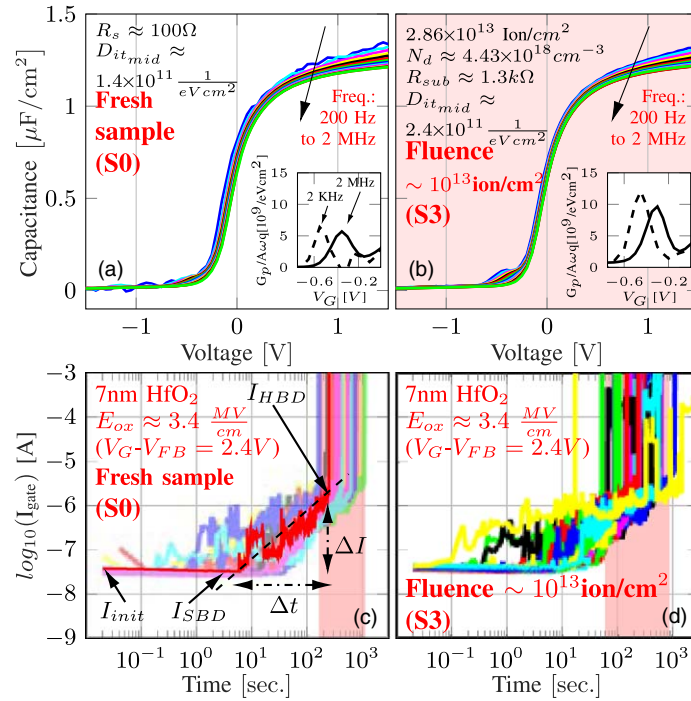
Fig. 2. (Color online) (a), (b) MFCV analyses of the fresh (S0) and highly irradiated sample (S3) showing negligible change in the D_{it}, as indicated by the negligible increase in the normalized parallel conductance (GP) shown in the insets. (c), (d) Gate current evolution from SBD to PBD, finally leading to HBD in a few devices of sample S0 and S3.
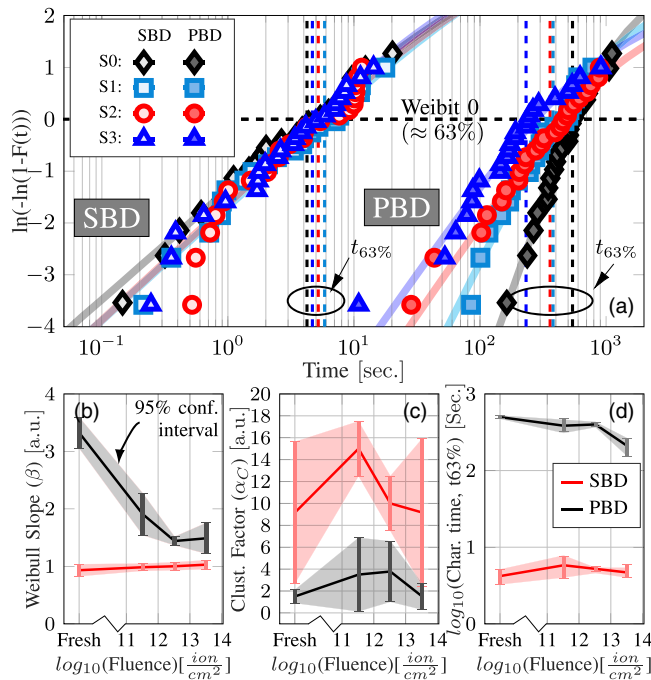

Fig. 3. (Color online) (a) Cluster model fitting on a Weibull plot to the SBD and PBD time durations in the HK-IL stack for samples S0–S3. Trend of (b) β, (c) α_C and (d) η for the diff. samples analyzed separately for SBD and PBD. In (b)–(d) the 95% confidence interval is indicated for each parameter estimate.

decline from 3 to 1.3. The unchanged values of β_{SBD} and our C–V evidence of radiation fluence only impacting the HK leads us to infer here that IL must be the first layer to suffer BD. The drastic reduction of β_{PBD} for higher fluence again reaffirms the fact that the second layer to percolate was HfO$_2$.

The cluster factor (α_C) is one of the most distinctive metrics that can help differentiate between HfO$_2$ and SiO$_X$.

Density functional theory (DFT) studies have convincingly shown that spatial clustering of defects is only prevalent in HfO$_2$ while it is almost non-existent in SiO$_X$.[20] The abnormally high values of $\alpha_{C\text{-}SBD} \sim 8\text{–}16$ clearly indicate no spatial defect correlation at all, which is only plausible if the SBD occurred in the IL layer (given the DFT evidence). The corresponding low values of $\alpha_{C\text{-}PBD} \sim 1.5\text{–}2$ again indicate significant correlation of defect generation in the second dielectric, which must correspond to percolation in the HfO$_2$ layer here.

Looking into the trend of η, we see that $\eta_{SBD} \ll \eta_{PBD}$. If we compute the field distribution in IL and HK using Gauss law (assuming zero surface charge), we can confirm that the field across IL layer is 6–7X of that in the HK. As such, the defect generation rate is several orders higher in the IL, which further confirms the claim of IL-first BD. Note that $\beta_{SBD} \ll \beta_{PBD}$ for sample S0 also provides further support to this conclusion as according to percolation theory, β is proportional to number of additional stress induced defects needed to initiate BD.

A final comment is worth to be made regarding the statistical significance of the results presented here. Given that according to the simulation-based approach presented by Yokogawa,[21] it is possible that β and α_C may be correlated; it could be argued that errors might be induced during the parameter estimation process in our study due to sparse data. Since common statistical significant tests used to check whether distributions are different generally require normality of the data distribution as a pre-requisite and focus only on the mean of the distributions[22] (such as the *t*-test), they are not suitable for the case under study here where our analysis is centered around β and α_C, not η. Instead, we focus on the 95% confidence interval of the parameter estimates. Note that even considering the maximum and minimum

values of the confidence intervals, the trends reported remain the same, that is: β decreases as a function of the radiation fluence for the PBD data but remains almost constant for the SBD trends, and α_C values are always higher for the SBD data than for the PBD data, suggesting a strongly clustered defect evolution phenomenon for the PBD data. Further studies are to be performed to experimentally explore the β and α_C correlation,[21] which requires measurement of a significant number of samples.

We have concluded through a holistic statistical investigation of the TDDB trends in a HfO$_2$—SiO$_X$ stack across SBD, PBD and HBD that the interfacial layer (SiO$_X$) is the first to break down, followed later by the HK. Our claim of the sequence of BD is based on the combined evidence from the trends of β, α_C and η for a wide range of radiation fluences. Our analysis here is accomplished with just a single device stack and a single stress condition leveraging on the careful design and tuning of the radiation strategy. Further study involving an in-depth probe into the spatio-temporal defect kinetics in the PBD phase using a defect centric multi-physics phonon trap-assisted tunneling model is currently under way and we hope that this will provide more insights into this kinetics.

The data that support the findings of this study are available from the corresponding author upon reasonable request.

ORCID iDs   Fernando Leonel Aguirre (iD) https://orcid.org/0000-0001-7793-1194   Alok Ranjan (iD) https://orcid.org/0000-0003-4592-1674   Nagarajan Raghavan (iD) https://orcid.org/0000-0001-6735-3108   Andrea Padovani (iD) https://orcid.org/0000-0003-1145-5257   Sebastián Matías Pazos (iD) https://orcid.org/0000-0002-7354-4530   Nahuel Vega (iD) https://orcid.org/0000-0002-0200-4588   Mario Debray (iD) https://orcid.org/0000-0002-2414-7547   Joel Molina-Reyes (iD) https://orcid.org/0000-0002-5681-1713   Kin Leong Pey (iD) https://orcid.org/0000-0002-0066-091X   Félix Palumbo (iD) https://orcid.org/0000-0002-7749-5035

1) L. Vandelli, A. Padovani, L. Larcher, G. Bersuker, J. Yum, and P. Pavan, 2011 IEEE Int. Reliability Physics Symp., 2011, p. GD.5.1.
2) V. Iglesias, M. Lanza, K. Zhang, A. Bayerl, M. Porti, M. Nafría, X. Aymerich, G. Benstetter, Z. Y. Shen, and G. Bersuker, Appl. Phys. Lett. **99**, 103510 (2011).
3) S. Lombardo, J. H. Stathis, B. P. Linder, K. L. Pey, F. Palumbo, and C. H. Tung, J. Appl. Phys. **98**, 121301 (2005).
4) N. Raghavan, K. L. Pey, and X. Li, Appl. Phys. Lett. **95**, 222903 (2009).
5) N. Raghavan, K. L. Pey, W. H. Liu, and X. Li, 2010 IEEE Int. Reliability Physics Symp., 2010, p. 778.
6) T. Nigam, A. Kerber, and P. Peumans, 2009 IEEE Int. Reliability Physics Symp., 2009, p. 523.
7) K. Okada, H. Ota, A. Hirano, A. Ogawa, T. Nabatame, and A. Toriumi, 2008 IEEE Int. Reliability Physics Symp., 2008, p. 661.
8) M. Rafik, G. Ribes, D. Roy, and G. Ghibaudd, J. Vac. Sci. Technol. B **27**, 472 (2009).
9) D. Y. Choi, K. Taek Lee, C.-K. Baek, C. Woo Sohn, H. Chul Sagong, E.-Y. Jung, J.-S. Lee, and Y.-H. Jeong, IEEE Electron Device Lett. **32**, 1319 (2011).
10) T. Kauerauf, R. Degraeve, E. Cartier, C. Soens, and G. Groeseneken, IEEE Electron Device Lett. **23**, 215 (2002).
11) A. Padovani, N. Raghavan, L. Larcher, and K. L. Pey, IEEE Electron Device Lett. **34**, 1289 (2013).
12) G. Bersuker et al., 2008 IEEE Int. Electron Devices Meeting, 2008, p. 1.
13) A. Barranco, F. Yubero, J. P. Espinós, P. Groening, and A. R. González-Elipe, J. Appl. Phys. **97**, 113714.1 (2005).
14) G. Knoll, Radiation Detection and Measurement (Wiley, New York, 2013).
15) R. Winter, J. Ahn, P. C. McIntyre, and M. Eizenberg, J. Vac. Sci. Technol. B **31**, 030604 (2013).
16) E. H. Nicollian and J. R. Brews, MOS (Metal Oxide Semiconductor) Physics and Technology (Wiley, New York, 2003).
17) S. Tous, E. Y. Wu, and J. Suñé, IEEE Electron Device Lett. **29**, 949 (2008).
18) N. Raghavan, A. Padovani, X. Wu, K. Shubhakar, M. Bosman, L. Larcher, and K. L. Pey, 2013 IEEE Int. Reliability Physics Symp. (IRPS), 2013, p. 5A.3.1.
19) E. Y. Wu, B. Li, J. H. Stathis, and C. LaRow, 2014 IEEE Int. Reliability Physics Symp., 2014, p. 5B.2.1.
20) D. Z. Gao, J. Strand, M. S. Munde, and A. L. Shluger, Front. Phys. **7**, 1 (2019).
21) S. Yokogawa, Jpn. J. Appl. Phys. **59**, SL0802 (2020).
22) D. C. Montgomery and G. C. Runger, Applied Statistics and Probability for Engineers (Wiley, New York, 2010).